Experimental and Molecular Pathology 107 (2019) 68–76

Contents lists available at ScienceDirect

Experimental and Molecular Pathology

journal homepage: www.elsevier.com/locate/yexmp

Propofol suppresses proliferation and migration of papillary thyroid cancer cells by down-regulation of lncRNA ANRIL

Fumei Chen[1], Mengyuan Li[1], Xiaoping Zhu*

Department of Anesthesiology, The First Affiliated Hospital of Nanchang University, Nanchang 330006, Jiangxi, China

ARTICLE INFO

Keywords:
Propofol
Papillary thyroid cancer
LncRNA ANRIL
Proliferation
Apoptosis
Migration

ABSTRACT

Background: Propofol is a popular anesthetic agent, with potent anti-tumor activity against many cancers. The objective of this study was to explore the potential effect of propofol on papillary thyroid cancer (PTC) in vitro.
Methods: Human PTC cell lines TPC-1 and IHH-4 were treated by propofol. ANRIL expression vector (pc-ANRIL) was transfected into TPC-1 cells to overexpress the expression of ANRIL. CCK-8, BrdU assay, transwell assay, flow cytometry and Western blot were performed to evaluate cell proliferation, migration and apoptosis. The expression changes of ANRIL were detected by RT-qPCR.
Results: Propofol with a concentration of 6 μg/mL significantly reduced TPC-1 and IHH-4 cells proliferation and migration, and significantly induced apoptosis. However, 6 μg/mL of propofol had no significant impacts on the proliferation and apoptosis of normal human thyroid follicular epithelial Nthy-ori 3–1 cells. Meanwhile, the expression of ANRIL in TPC-1 cells was down-regulated by propofol. The anti-tumor activity of propofol was attenuated when ANRIL was overexpressed. Additionally, propofol blocked Wnt/β-catenin and NF-κB pathways in an ANRIL-dependent fashion.
Conclusion: Our findings suggested the in vitro anti-tumor potential of propofol in PTC. One possible mechanism involved in the anti-tumor activity was preliminary revealed: propofol down-regulated the expression of ANRIL, and thus blocking Wnt/β-catenin and NF-κB pathways.

1. Introduction

Thyroid cancer is the most common endocrine cancer, and is the top five most common cancers that occur in women. The incidence rates are 3-fold higher in women than in men, i.e., 21 vs. 7 per 100,000 population (Siegel et al., 2017). Papillary thyroid cancer (PTC) is one type of thyroid cancer, accounting for > 80% of thyroid cancers (Bokhari and Tiscornia-Wasserman, 2017). Patients with PTC always have a good prognosis, but PTC patients with aggressive features, such as large primary tumor, extra-thyroidal invasion, lymph node metastasis, advanced tumor-node-metastasis stage or recurrences, have an unsatisfied prognosis (Voutilainen et al., 2001).

Propofol (2,6-disopropylphenol) is a popular drug that is recommended for anaesthesia in surgery and for sedation in intensive care units (ICUs) (Krajcova et al., 2015). The mechanisms of action on the central nervous system are associated with GABA receptors and inhibitory effects of the neurotransmitter (Folino and Parks, 2018). Compared with other anesthetic agents, propofol has many pharmacological advantages, such as quick onset, quick offset, high-quality recovery, and few side-effects (Chidambaran et al., 2015). Besides, it has been found that propofol exerted a number of non-anesthetic effects, including anti-apoptotic (Zhao and Zhang, 2018), anti-oxidative (Shinjo and Tanaka, 2018), immunomodulatory (Peng et al., 2014), and anti-tumor (Wang et al., 2018a; Xu et al., 2018) activities. Particularly in human cancers, propofol has been reported to exhibit potent anti-tumor activity in a wide range of cancer cell lines, including cervical cancer cell line Hela (Chen et al., 2018a), colorectal cancer cell lines HT29, SW480 and RKO (Chen et al., 2018b; Xu et al., 2018), lung cancer cell line A549 (Liu and Liu, 2018), breast cancer cell line MDA-MB-435 (Yu et al., 2018) and etc. However, the effects of propofol on thyroid cancer have not been studied yet.

Long noncoding RNAs (lncRNAs) are noncoding transcripts with length longer than 200 nucleotides. Although they have no protein-coding capacity, increasing evidence suggested that lncRNAs participate in almost all cellular processes (Li et al., 2016; Yang et al., 2017). In particular, several lncRNAs have been identified as promising

* Corresponding author at: Department of Anesthesiology, The First Affiliated Hospital of Nanchang University, No.17, Yongwaizheng Street, Donghu District, Nanchang 330006, Jiangxi, China.
E-mail address: xiaopingzhu011@sina.com (X. Zhu).
[1] Co-first authors.

https://doi.org/10.1016/j.yexmp.2019.01.011
Received 2 August 2018; Received in revised form 13 November 2018; Accepted 26 January 2019
Available online 28 January 2019
0014-4800/

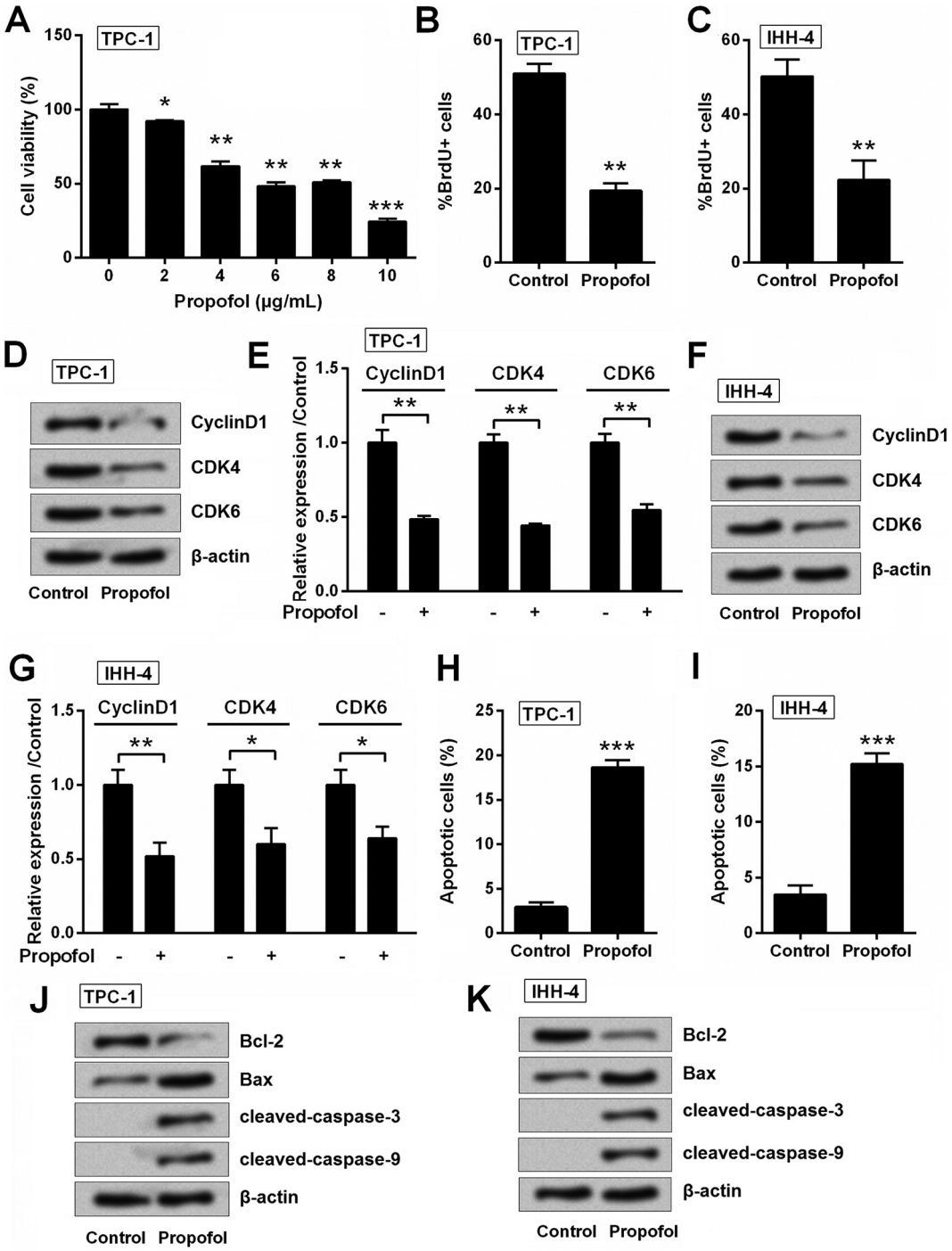

Fig. 1. Propofol inhibits PTC cells proliferation and promotes apoptosis. (A) TPC-1 cells were exposed to various doses of propofol for 48 h, and then the viability was measured by CCK-8 assay. TPC-1 and IHH-4 cells were treated by 6 μg/mL propofol for 48 h, and then (B–C) cell proliferation, (D–G) cell cycle-related protein expression, (H–I) apoptotic cell rate, and (J-K) apoptosis-related protein expression were evaluated by BrdU assay, Western blot, and flow cytometry detection. $^{*}P < .05$, $^{**}P < .01$, and $^{***}P < .001$.

prognostic markers, and some of which functioned as anti-oncogenes or oncogenes (Liu et al., 2016; Murugan et al., 2018). Antisense noncoding RNA in the *INK4* locus (ANRIL) is an lncRNA, which is initially found in patients with familial melanoma-neural system tumor (Pasmant et al., 2007). It is transcribed in the antisense orientation of the *INK4B-ARF-INK4A* gene cluster, to generate a 3834-nt RNA consisting of 19 exons (Tano and Akimitsu, 2012). Many studies have demonstrated that ANRIL plays an oncogenic role in several cancers, including oral (Chai et al., 2018), prostate (Zhao et al., 2018), and breast cancers (Xu et al., 2017). Another study pointed out that ANRIL was highly expressed in thyroid cancer, and silence of ANRIL inhibited thyroid cancer cells proliferation, invasion and metastasis (Zhao et al., 2016). Those previous findings together suggested that ANRIL was a typical oncogene.

This is an in vitro study performed in human PTC cell lines (TPC-1 and IHH-4), to reveal the effects of propofol on PTC cells proliferation, apoptosis, and migration. We also studied the regulatory role of propofol in ANRIL expression in order to decode one possible mechanism of propofol's action.

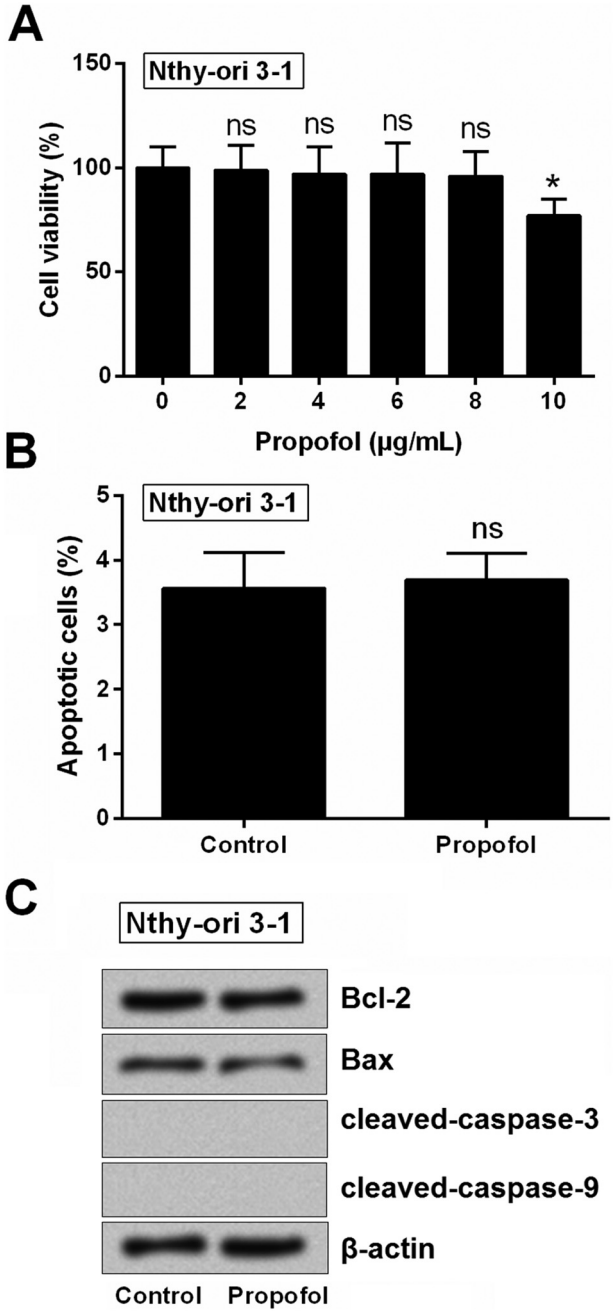

Fig. 2. Low doses of propofol cannot impact Nthy-ori 3–1 cells proliferation and apoptosis. (A) Nthy-ori 3–1 cells were treated by various doses of propofol for 48 h, and then the viability was measured by CCK-8 assay. Nthy-ori 3–1 cells were treated by 6 μg/mL propofol for 48 h, and then (B) apoptotic cell rate and (C) apoptosis-related protein expression were evaluated by flow cytometry detection and Western blot respectively. ns, no significant; *$P < .05$.

2. Materials and methods

2.1. Cell culture and treatment

Human PTC cell line TPC-1 and IHH-4 were respectively purchased from the Type Culture Collection of the Chinese Academy of Sciences (Shanghai, China) and Japanese Collection of Research Bioresources (JCRB) cell bank (Osaka, Japan). Normal human thyroid follicular epithelial Nthy-ori 3–1 cell line was obtained from European Collection of Cell Cultures (ECACC, Porton Down, UK). TPC-1 cells were cultured in low-glucose Dulbecco's Modified Eagle Medium (DMEM, Gibco, Grand Island, NY, USA) supplementing with 10% heat-inactivated fetal bovine serum (FBS, Gibco). IHH-4 and Nthy-ori 3–1 cells were cultured in Roswell Park Memorial Institute (RPMI)-1640 medium (Gibco) supplemented with 10% FBS (Gibco), 0.1 mM non-essential amino acids (Sigma-Aldrich, St. Louis, MO, USA), and 1 mM sodium pyruvate (Sigma-Aldrich). All cells were maintained at 37 °C in a humidified atmosphere with 5% CO_2.

British Pharmacopoeia (BP) Reference Standard propofol was purchased from Sigma-Aldrich. Propofol was dissolved in DMSO (Sigma-Aldrich) and was made up with the culture medium until the final concentration of DMSO was < 0.1%. Cells were treated by 0–10 μg/mL of propofol for 48 h. The cells treated by same volume of vehicle were used as blank controls.

2.2. Cell transfection

Human ANRIL sequence was inserted into pcDNA3.1 plasmid (Invitrogen, Carlsbad, CA, USA) to construct an ANRIL expression vector (pc-ANRIL). The empty pcDNA3.1 was used as a blank control. pc-ANRIL and pcDNA3.1 was transfected into TPC-1 cells with the help of lipofectamine 3000 reagent (Life Technologies Corporation, Carlsbad, CA, USA). Transfection was performed for 48 h in 6-well plates under serum-free and antibiotics-free conditions. Transfection efficiency was verified by RT-qPCR.

2.3. Cell viability assessment

The transfected or untransfected cells (5×10^3) were seeded in 96-well plates and were incubated at 37 °C overnight. Propofol or vehicle was added into cells, and the plates were further incubated for 48 h to assay cell viability. Ten microliter CCK-8 solution (Dojindo Molecular Technologies, Kyushu, Japan) was added, and the plates were incubated at 37 °C for 4 h. The absorbance of each well was read by using a Microplate Reader (Bio-Rad, Hercules, CA) at a wavelength of 450 nm.

2.4. BrdU assay

The sterile coverslip was placed in 24-well plates, and 5×10^4 transfected or untransfected cells were added into each well. Until the confluence reached 50–60%, the cells were treated by propofol or vehicle for 48 h. Thereafter, 10 μM BrdU solution (Solarbio, Beijing, China) was added and the plates were further incubated for 4 h. Followed by fixing in 4% cold paraformaldehyde for 20 min and permeabilizing by 0.2% Triton X-100 for 10 min, the cells were probed by anti-BrdU monoclonal antibody (1: 500, Cat: K006322P, Solarbio). Cell nucleus was stained by 0.5 μg/mL of DAPI (Sigma-Aldrich). The stained cells in the coverslips were counted under a fluorescence microscopy (IX70, Olympus, Tokyo, Japan).

2.5. Apoptosis assay

Annexin V-FITC Apoptosis Detection Kit purchased from Beyotime (Shanghai, China) was utilized in this study for testing apoptotic cells (Annexin V-FITC-positive and PI-negative). The transfected or untransfected cells (5×10^5) were seeded in 6-well plates. Until the confluence reached 70–80%, cells were treated by propofol or vehicle for 48 h. Thereafter, cells were collected by trypsin (Sigma-Aldrich) and centrifugation. 1×10^5 cells from each sample were resuspended in 200 μL Binding Buffer containing 5 μL Annexin V-FITC and 10 μL PI. After incubation at room temperature for 20 min in the dark, apoptotic cells were distinguished by a FACS can (Beckman Coulter, Fullerton, CA, USA). The rate of apoptotic cells was calculated by using FlowJo software (Treestar, San Carlos, CA, USA).

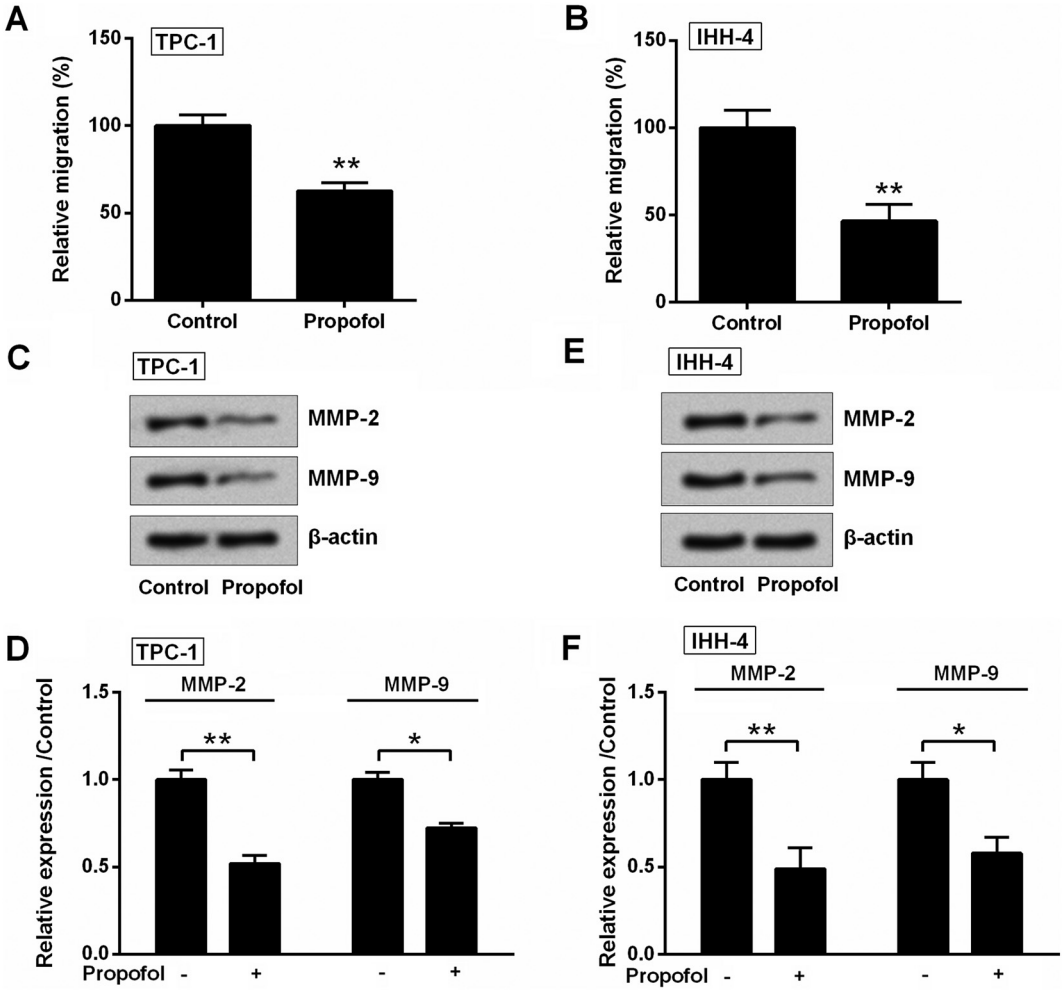

Fig. 3. Propofol inhibits PTC cells migration. TPC-1 and IHH-4 cells were treated by 6 μg/mL propofol for 48 h. (A–B) Relative migration, and (C–F) the protein expression of MMPs were respectively assessed by transwell assay and Western blot. *$P < .05$, and **$P < .01$.

2.6. Transwell migration assay

A HTS Transwell® 24-well Permeable Support (Corning, New York, USA) with polyester (PET) membrane (0.4 μm pore size) was used in this study for migration assay. The transfected or nontransfected cells were starved in non-serum culture medium for 12 h, and were collected by trypsin (Sigma-Aldrich) and centrifugation. 1×10^5 cells per mL in 200 μL non-serum culture medium with propofol or vehicle was added into the upper chamber. The lower chamber was filled with 600 μL completed culture medium. After 48 h of incubation at 37 °C, the cells in the upper chamber were removed by cotton swab, and the cells in the lower side were stained by 0.5% crystal violet (Betotime) at room temperature for 5 min. The stained cells in the five randomly selected fields were counted microscopically.

2.7. RT-qPCR

Isolation of RNAs from TPC-1 cells was performed by using the mirVana PARIS Kit (Ambion, Austin, TX, USA), according to the manufacturer's instructions. The RNA yield was calculated using spectrophotometry, and 2 μg total RNA was reversely transcribed into cDNA by using PrimeScript™ RT reagent kit with gDNA Eraser (Takara, Dalian, China). qPCR for testing of ANRIL was performed in a 20-μL reaction volume by using SYBR® Premix Ex TagTM II (Takara). The expression of ANRIL was normalized to GAPDH, and was calculated according to the $2^{-\Delta\Delta Ct}$ method.

2.8. Western blot

Cellular protein was isolated by using RIPA lysis buffer (Beyotime). The protein yield was calculated by using Enhanced BCA Protein Assay Kit (Beyotime). 40 μg whole-cell extracts were separated by SDS-PAGE and were transferred onto PVDF membranes (Millipore). After incubated at Western Blocking Buffer (Beyotime) for 1 h at room temperature on rotary shaker, the proteins in membranes were probed by primary antibodies at 4 °C, overnight for the detection of: CyclinD1 (ab40754, Abcam, Cambridge, MA), CDK4 (ab137675), CDK6 (ab151247), Bcl-2 (ab196495), Bax (ab32503), cleaved-caspase-3 (ab13847), cleaved-caspase-9 (ab2324), MMP-2 (ab97779), MMP-9 (ab38898), Wnt3a (ab19925), β-catenin (ab16051), p-IκBα (ab133462), IκBα (ab32518), p-p65 (ab86299), p65 (ab32536), and β-actin (ab8227). The membranes were then incubated with the secondary antibodies for 1 h at room temperature. BeyoECL Plus kit (Beyotime) was used to make the protein bands visible and the intensity of the bands was quantified using Image Lab™ Software (Bio-Rad, Hercules, CA, USA).

2.9. Statistical analysis

Three replicates of each group were analyzed, and detection on each replicate was performed in triplicate. Data were represented as mean ± SD. Statistical differences between groups were analyzed on SPSS 19.0 (Chicago, IL, USA) by ANOVA (following with Duncan post-

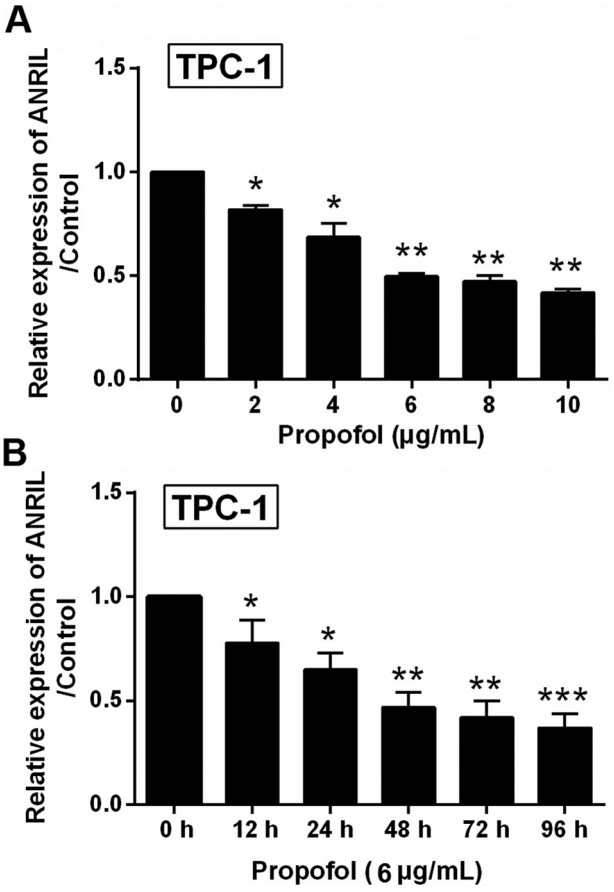

Fig. 4. Propofol down-regulates the expression of ANRIL. (A) TPC-1 cells were exposed to various doses of propofol for 48 h. (B) TPC-1 cells were exposed to 6 μg/mL propofol for various times. The expression changes of ANRIL were determined by RT-qPCR. *$P < .05$, **$P < .01$, and ***$P < .001$.

hoc) or Student-*t*-test. *P*-values lower than 0.05 were considered to indicate statistical significance.

3. Results

3.1. Propofol inhibits PTC cells proliferation and promotes apoptosis

In the beginning, TPC-1 cells were exposed to various doses of propofol for 48 h, and the viability inhibition was observed in Fig. 1A. The viability was significantly reduced to 48.31% by 6 μg/mL of propofol, thus 6 μg/mL was selected as a propofol-treating condition for use in the following investigations. Then, the effects of propofol on the proliferation and apoptosis of two human PTC cell lines (TPC-1 and IHH-4) were assessed. Fig. 1B–C showed that, BrdU-positive cell rates were much lower in propofol group than the control group ($P < .01$). By performing Western blot analysis, the down-regulations of CyclinD1, CDK4 and CDK6 were observed in propofol group than the control group ($P < .05$ or $P < .01$, Fig. 1D–G). In addition, Fig. 1H–I showed that, apoptotic cell rates were significantly increased in propofol group as compared to the control group ($P < .001$). To support the induction of apoptosis, Western blot analysis was carried out and results in Fig. 1J–K showed that propofol remarkably down-regulated Bcl-2 expression, up-regulated Bax expression, and clearly cleaved caspase-3 and -9. These data suggested that propofol could effectively inhibit the growth of TPC-1 and IHH-4 cells by inhibiting proliferation and inducing apoptosis.

Next, the effects of propofol on the proliferation and apoptosis of normal human thyroid follicular epithelial Nthy-ori 3–1 cell line were measured, to see whether propofol affected PTC cells specifically. Data in Fig. 2A showed that, the viability of Nthy-ori 3–1 cells was significantly reduced by 10 μg/mL of propofol ($P < .05$). However, propofol with concentrations less than or equal to 8 μg/mL could not impact Nthy-ori 3–1 cells viability significantly ($P > .05$). Then, Nthy-ori 3–1 cells were treated by 6 μg/mL of propofol, and cell apoptosis was tested. Results in Fig. 2B displayed that apoptotic cell rate was unchanged after treatment with propofol ($P > .05$). This phenomenon was confirmed by the results from Western blot analysis, as shown in Fig. 2C, no alterations of Bcl-2, Bax, cleaved-caspase-3 and cleaved-caspase-9 were observed between propofol and control groups. All these data suggested that low concentration of propofol could not impact Nthy-ori 3–1 cells survival, but could inhibit PTC cells survival.

3.2. Propofol inhibits PTC cells migration

Effects of propofol on TPC-1 and IHH-4 cells migration were detected. As shown in Fig. 3A–B, relative migration was significantly reduced in propofol group as compared to the control group ($P < .01$). Meanwhile, protein levels of MMP-2 and MMP-9 were significantly down-regulated in propofol group as compared to the control group ($P < .01$ and $P < .05$, Fig. 3C–F). These data suggested that propofol could inhibit the migratory capacity of PTC cells.

3.3. Propofol down-regulates the expression of ANRIL

The expression changes of ANRIL in response to propofol treatment were preliminarily studied in TPC-1 cells. RT-qPCR data in Fig. 4A–B displayed that, the expression of ANRIL was significantly reduced in propofol group as compared to the untreated group ($P < .05$, $P < .01$ or $P < .001$). Besides, propofol inhibited ANRIL expression possibly in both dose- and time-dependent manner, as a higher dose of propofol induced a lower ANRIL expression (Fig. 4A), and ANRIL expression was decreased with the time increasing (Fig. 4B). Thus, ANRIL might be one of the downstream effectors of propofol.

3.4. Propofol inhibits TPC-1 cells proliferation and promotes apoptosis via down-regulating ANRIL

Whether the down-regulation of ANRIL was a reason for the effects of ANRIL on propofol-treated TPC-1 cells was subsequently investigated. Fig. 5A showed that, ANRIL expression was significantly increased by pc-ANRIL transfection when compared with pcDNA3.1 transfection ($P < .01$), suggesting ANRIL-overexpressing cells were successfully established. More importantly, the viability and BrdU-positive cell rate were significantly increased (both $P < .05$, Fig. 5B–C), and cell cycle-related proteins were significantly up-regulated ($P < .01$ or $P < .001$, Fig. 5D–E) in propofol + pc-ANRIL group, as compared to propofol + pcDNA3.1 group. Also, the apoptotic cell rate was significantly reduced ($P < .05$, Fig. 5F), Bcl-2 was up-regulated, Bax was down-regulated, and the cleavage of caspase-3 and -9 was repressed (Fig. 5G) in propofol + pc-ANRIL group as compared to propofol + pcDNA3.1 group.

3.5. Propofol inhibits TPC-1 cells migration via down-regulating ANRIL

Next, whether ANRIL down-regulation contributed to propofol-altered cell migration was tested. As a result, relative migration was significantly increased ($P < .05$, Fig. 6A) and the expression levels of MMP-2 and MMP-9 were up-regulated (both $P < .001$, Fig. 6B–C) in propofol + pc-ANRIL group, as compared to propofol + pcDNA3.1 group.

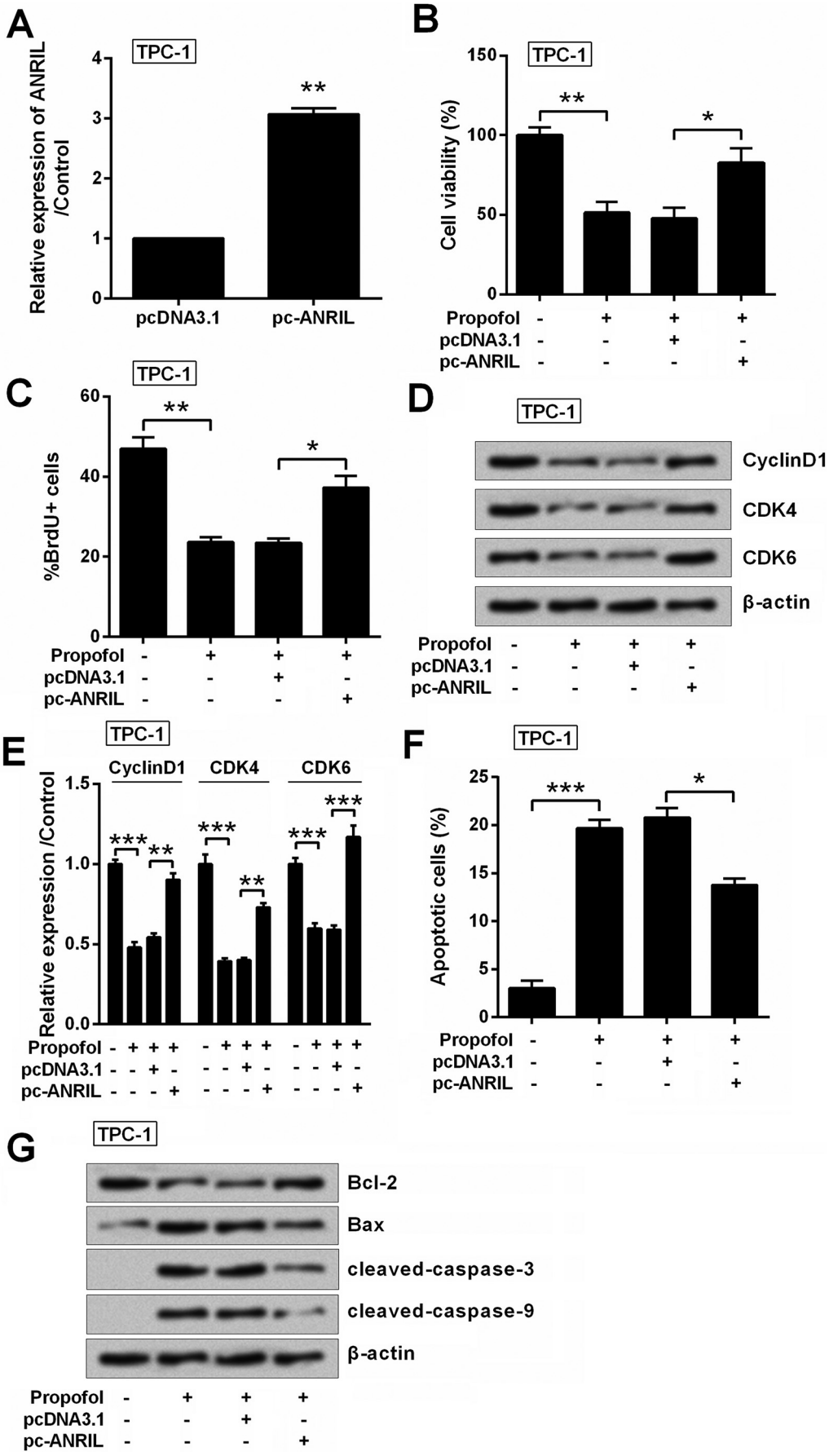

(caption on next page)

Fig. 5. Propofol inhibits TPC-1 cells proliferation and promotes apoptosis via down-regulating ANRIL. TPC-1 cells were transfected with pc-ANRIL or pcDNA3.1, and then were treated by 6 μg/mL propofol for 48 h. (A) Transfection efficiency was verified by RT-qPCR. (B) Cell viability, (C) proliferation, (D-E) cell cycle-related protein expression, (F) apoptotic cell rate, and (G) apoptosis-related protein expression were evaluated by CCK-8 assay, BrdU assay, Western blot, and flow cytometry detection. *$P < .05$, **$P < .01$, and ***$P < .001$.

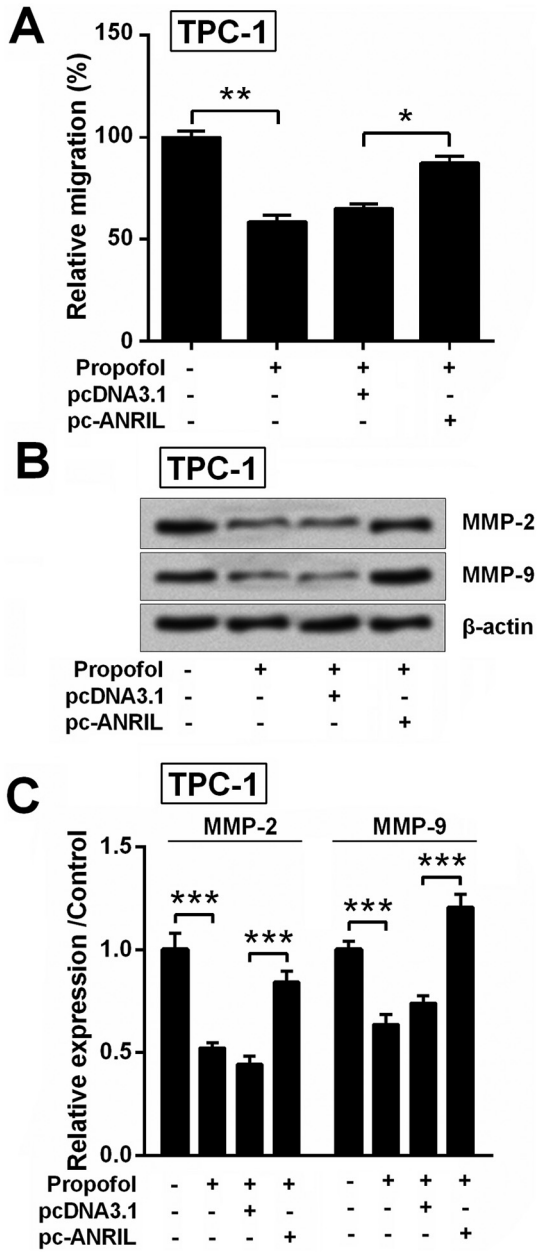

Fig. 6. Propofol inhibits TPC-1 cells migration via down-regulating ANRIL. TPC-1 cells were transfected with pc-ANRIL or pcDNA3.1, and then were treated by 6 μg/mL propofol for 48 h. (A) Relative migration, and (B–C) the protein expression of MMPs were respectively assessed by transwell assay and Western blot. *$P < .05$, **$P < .01$, and ***$P < .001$.

3.6. Propofol represses Wnt/β-catenin and NF-κB pathways via down-regulating ANRIL

We finally explored the underlying pathways of which propofol conferred its anti-tumor activities. Fig. 7A–D showed that, propofol significantly down-regulated the protein levels of Wnt3a and β-catenin, as well as the phosphorylation levels of IκBα and p65 ($P < .05$ or $P < .01$). Compared with propofol + pcDNA3.1 group, the protein levels of Wnt3a and β-catenin, and the phosphorylation levels of IκBα and p65 were significantly up-regulated in propofol + pc-ANRIL group ($P < .01$ or $P < .001$).

4. Discussion

The main findings of this study are that 6 μg/mL of propofol significantly reduced TPC-1 and IHH-4 cells proliferation and migration, and significantly induced apoptosis. However, 6 μg/mL of propofol had no significant impacts on the proliferation and apoptosis of normal human thyroid follicular epithelial Nthy-ori 3–1 cells. Meanwhile, propofol down-regulated the expression of ANRIL in TPC-1 cells in both time- and dose-dependent manner. And the down-regulated ANRIL by propofol contributed to the anti-tumor activities of propofol, as the impacts of on TPC-1 cells proliferation, migration and apoptosis were attenuated when ANRIL was overexpressed. Additionally, propofol blocked Wnt/β-catenin and NF-κB pathways, while ANRIL overexpression reactivated these two signaling in propofol-treated cell.

Propofol is one of the most commonly used anesthetic agents which is recommend for use in ICUs or during surgery. In addition to its anesthetic effect, the anti-tumor effect of propofol has attracted increasing attention (Chen et al., 2018a; Chen et al., 2018b; Liu and Liu, 2018; Wang et al., 2018a; Xu et al., 2018; Yu et al., 2018). Herein, we explored the effects of propofol on human PTC cell lines (TPC-1 and IHH-4) in vitro, which was unstudied before. We found that propofol with a concentration of 6 μg/mL significantly reduced BrdU-positive cell rate in TPC-1 and IHH-4 cells, indicating the anti-proliferating effects of propofol in TPC-1 cells. We additionally found that propofol suppressed the expression of CyclinD1, CDK4 and CDK6. Cell cycle is regulated by different cyclin/CDK complexes. CyclinD1 is a key regulator of CDK4 and CDK6, whose activity is required for cell cycle G1/S transition (Galderisi et al., 2003). These evidences suggested that propofol suppressed TPC-1 and IHH-4 cells proliferation via alteration of cell cycle, arresting cells in G1 phase. Moreover, the pro-apoptotic effect of propofol was observed on TPC-1 and IHH-4 cells, and the apoptosis induced by propofol probably through a mitochondia-dependent pathway, as the balance between Bcl-2 and Bax was disrupted.

Most PTC patients have a good prognosis, but this kind of cancer has a high propensity for lymph node metastasis (Sancho et al., 2014), which significantly reduces the prognosis of patients with aggressive PTC (Voutilainen et al., 2001). Migration is one important parameter in evaluating cancer cells metastasis. This study revealed that propofol significantly reduced the relative migration of TPC-1 and IHH-4 cells. Besides, the protein levels of MMP-2 and MMP-9 were remarkably down-regulated in response to propofol treatment. MMPs are proteolytic enzymes responsible for remodeling extracellular matrix (ECM) (Kessenbrock et al., 2010). MMPs also represent the most prominent family of proteinases associated with tumorigenesis by controlling of tumor growth, metastasis and angiogenesis (Kessenbrock et al., 2010). MMP-2 and MMP-9 are two of the best characterized members of MMP family, and play significant roles in collagen degradation (Kapelko-Slowik et al., 2018). Previous studies have demonstrated the inhibitory effects of propofol on several kinds of cancer cells migration and invasion via modulation of MMP-2 and MMP-9 (Huang et al., 2016; Xu et al., 2013). However, our finding for the first time revealed the inhibitory effect of propofol on PTC cells migration was partly due to the down-regulation of MMP-2 and MMP-9.

Recently, a growing number of evidences have suggested that genetic deregulation of lncRNAs results in activation of divers signaling pathways that drive the cells for uncontrolled cell growth and metastasis in thyroid cancer (Ding et al., 2018; Wang et al., 2018b). By

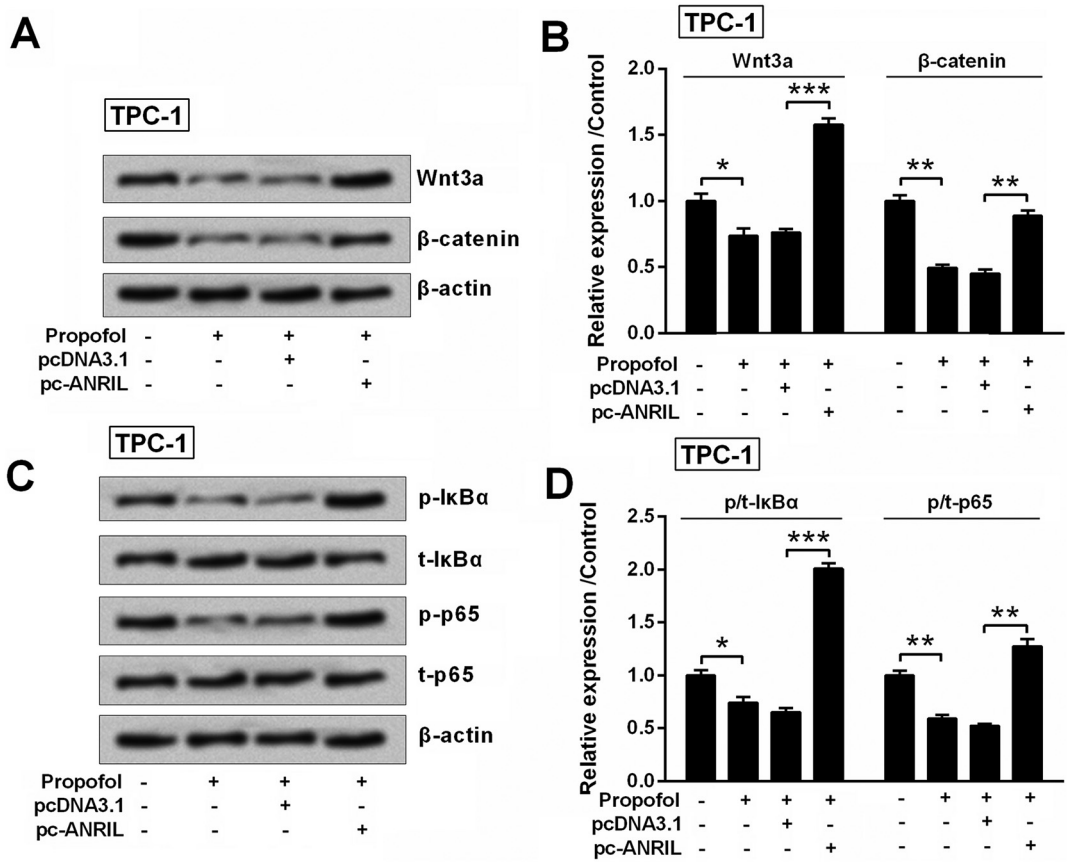

Fig. 7. Propofol represses Wnt/β-catenin and NF-κB pathways via down-regulating ANRIL. TPC-1 cells were transfected with pc-ANRIL or pcDNA3.1, and then were treated by 6 μg/mL propofol for 48 h. Protein expression changes of core factors in (A-B) Wnt/β-catenin and (C-D) NF-κB pathways were tested by Western blot. $^{*}P < .05$, $^{**}P < .01$, and $^{***}P < .001$.

performing RNA-sequencing analysis, a total of 146 lncRNAs were differentially expressed in hippocampus following propofol treatment (Fan et al., 2018). However, to our best of knowledge, the relationship between propofol and lncRNA in cancer cells has only been mentioned in one report (Zhang et al., 2015). This here, we found that propofol significantly down-regulated ANRIL expression in TPC-1 cells. This finding suggested that ANRIL is constitutively expressed in TPC-1 cells, but whether it is commonly expressed in other types of cells is still unclear, which need to be further studied. We additionally found that, ANRIL down-regulation conferred the anti-tumor activities of propofol. This finding was consistence with a previous study in which the oncogenic role of ANRIL in thyroid cancer has been mentioned (Zhao et al., 2016).

Wnt/β-catenin is an important pathway in regulating cancer initiation and progression (Sastre-Perona and Santisteban, 2012). Activation of the Wnt/β-catenin pathway promotes tumor growth in the thyroid (Reya and Clevers, 2005). The Wnt family comprises 19 human proteins, among which Wnt3a is involved in canonical Wnt pathway. Wnt3a can induce the accumulation of β-catenin, a key switch in the canonical Wnt pathway, and thus play key roles in regulating pleiotropic cellular functions (He et al., 2015). Several groups have suggested a strong correlation between cytoplasmic β-catenin and CyclinD1 expression in PTC (Ishigaki et al., 2002; Meirmanov et al., 2003). In the current study, a significant down-regulation of CyclinD1 following propofol treatment was observed in TPC-1 cells. Thus, we further studied the regulatory effect of propofol on Wnt/β-catenin pathway. In addition to Wnt/β-catenin, NF-κB pathway has also been reported to play a role in thyroid malignancies for its ability in controlling thyroid neoplastic cells proliferation and apoptosis (Pacifico and Leonardi, 2010). p65, RelB, c-Rel, NF-κB1 and NF-κB2 are five members of NF-κB family. p65 contains C-terminal transaction domain, which is essential for transcriptional activity. Besides, activation of NF-κB generally occurs by release from the IκB molecules (Hoesel and Schmid, 2013). Thus, in this study, Wnt3a, β-catenin, p65 and IκBα were selected as markers to evaluate the activity of Wnt/β-catenin and NF-κB pathways. We found that propofol blocked Wnt/β-catenin and NF-κB pathways in an ANRIL-dependent fashion, indicating the anti-tumor activity of propofol was partly due to regulating ANRIL, which further modulated Wnt/β-catenin and NF-κB signaling pathways.

To date, lncRNAs have been reported as key regulators in multiple cellular processes, but how lncRNAs work is still unclear. One possible hypothesis has been proposed, in which lncRNAs act as molecular sponges for miRNAs by binding effects, in having miRNAs exhausted, and finally separating the targeted mRNAs from binding with miRNAs. Such lncRNAs are called competing endogenous RNAs (ceRNAs). Recently, studies have evidenced that ANRIL appeared to act as a sponge for several miRNAs, such as miR-125a (Li et al., 2017), Let-7a (Zhang et al., 2018), and miR-199a (Xu et al., 2017). Thus, we inferred that ANRIL activated NF-κB and Wnt/β-catenin signaling pathways possibly via regulating miRNAs. However, which miRNAs are involved in the regulation between ANRIL and signaling pathways still need to be further studied. Besides, considering oncogenic proteins RET/PTC, RAS and BRAF, are involved in many aspects of thyroid carcinogenesis and are responsible for activation of NF-κB pathway (Coperchini et al., 2016; Pacifico and Leonardi, 2010), further investigations are required to reveal the link between propofol and RET/PTC expression.

5. Conclusions

In conclusion, our findings suggested the anti-tumor potential of

propofol in PTC. And also, we revealed one possible mechanism of action: propofol down-regulated the expression of ANRIL, and thus blocking Wnt/β-catenin and NF-κB pathways. Our data provided an in vitro evidence for the potential application of propofol in PTC treatment.

Funding

This research did not receive any specific grant from funding agencies in the public, commercial, or not-for-profit sectors.

Declarations of interest

None.

Acknowledgments

None.

References

Bokhari, A., Tiscornia-Wasserman, P.G., 2017. Cytology diagnosis of metastatic clear cell renal cell carcinoma, synchronous to pancreas, and metachronous to thyroid and contralateral adrenal: Report of a case and literature review. Diagn. Cytopathol. 45, 161–167.
Chai, L., et al., 2018. The role of long non-coding RNA ANRIL in the carcinogenesis of oral cancer by targeting miR-125a. Biomed. Pharmacother. 103, 38–45.
Chen, X., et al., 2018a. Propofol inhibits HeLa cells by impairing autophagic Flux via AMP-Activated Protein Kinase (AMPK) activation and endoplasmic reticulum stress regulated by calcium. Med. Sci. Monit. 24, 2339–2349.
Chen, X., et al., 2018b. Propofol disrupts aerobic glycolysis in colorectal cancer cells via inactivation of the NMDAR-CAMKII-ERK pathway. Cell. Physiol. Biochem. 46, 492–504.
Chidambaran, V., et al., 2015. Propofol: a review of its role in pediatric anesthesia and sedation. CNS Drugs 29, 543–563.
Coperchini, F., et al., 2016. Normal human thyroid cells, BCPAP, and TPC-1 thyroid tumor cell lines display different profile in both basal and TNF-alpha-induced CXCL8 secretion. Endocrine 54, 123–128.
Ding, S., et al., 2018. LncRNA SNHG12 promotes the proliferation and metastasis of papillary thyroid carcinoma cells through regulating wnt/beta-catenin signaling pathway. Cancer Biomark. 22, 217–226.
Fan, J., et al., 2018. Profiling of long non-coding RNAs and mRNAs by RNA-sequencing in the hippocampi of adult mice following propofol sedation. Front. Mol. Neurosci. 11, 91.
Folino, T.B., Parks, L.J., 2018. Propofol. StatPearls Publishing LLC, Treasure Island (FL).
Galderisi, U., et al., 2003. Cell cycle regulation and neural differentiation. Oncogene 22, 5208–5219.
He, S., et al., 2015. Wnt3a: functions and implications in cancer. Chin. J. Cancer 34, 554–562.
Hoesel, B., Schmid, J.A., 2013. The complexity of NF-kappaB signaling in inflammation and cancer. Mol. Cancer 12, 86.
Huang, X., et al., 2016. Propofol inhibits invasion and growth of ovarian cancer cells via regulating miR-9/NF-kappaB signal. Braz. J. Med. Biol. Res. 49, e5717.
Ishigaki, K., et al., 2002. Aberrant localization of beta-catenin correlates with overexpression of its target gene in human papillary thyroid cancer. J. Clin. Endocrinol. Metab. 87, 3433–3440.
Kapelko-Slowik, K., et al., 2018. Elevated serum concentrations of metalloproteinases (MMP-2, MMP-9) and their inhibitors (TIMP-1, TIMP-2) in patients with Graves' orbitopathy. Adv. Clin. Exp. Med. 27, 99–103.
Kessenbrock, K., et al., 2010. Matrix metalloproteinases: regulators of the tumor microenvironment. Cell 141, 52–67.
Krajcova, A., et al., 2015. Propofol infusion syndrome: a structured review of experimental studies and 153 published case reports. Crit. Care 19, 398.
Li, J., et al., 2016. Long noncoding RNAs regulate cell growth, proliferation, and apoptosis. DNA Cell Biol. 35, 459–470.
Li, R., et al., 2017. Knockdown of ANRIL aggravates H2O2-induced injury in PC-12 cells by targeting microRNA-125a. Biomed. Pharmacother. 92, 952–961.
Liu, W.Z., Liu, N., 2018. Propofol inhibits lung cancer A549 cells growth and epithelial-mesenchymal transition process by up-regulation of microRNA-1284. Oncol. Res. 27, 1–8.
Liu, F.T., et al., 2016. Long noncoding RNA ANRIL: a potential novel prognostic marker in cancer: a meta-analysis. Minerva Med. 107, 77–83.
Meirmanov, S., et al., 2003. Correlation of cytoplasmic beta-catenin and cyclin D1 overexpression during thyroid carcinogenesis around Semipalatinsk nuclear test site. Thyroid 13, 537–545.
Murugan, A.K., et al., 2018. Long noncoding RNAs: emerging players in thyroid cancer pathogenesis. Endocr. Relat. Cancer 25, R59–r82.
Pacifico, F., Leonardi, A., 2010. Role of NF-kappaB in thyroid cancer. Mol. Cell. Endocrinol. 321, 29–35.
Pasmant, E., et al., 2007. Characterization of a germ-line deletion, including the entire INK4/ARF locus, in a melanoma-neural system tumor family: identification of ANRIL, an antisense noncoding RNA whose expression coclusters with ARF. Cancer Res. 67, 3963–3969.
Peng, M., et al., 2014. Posttreatment with propofol attenuates lipopolysaccharide-induced up-regulation of inflammatory molecules in primary microglia. Inflamm. Res. 63, 411–418.
Reya, T., Clevers, H., 2005. Wnt signalling in stem cells and cancer. Nature 434, 843–850.
Sancho, J.J., et al., 2014. Prophylactic central neck disection in papillary thyroid cancer: a consensus report of the European Society of Endocrine Surgeons (ESES). Langenbeck's Arch. Surg. 399, 155–163.
Sastre-Perona, A., Santisteban, P., 2012. Role of the wnt pathway in thyroid cancer. Front. Endocrinol. (Lausanne) 3, 31.
Shinjo, T., Tanaka, T., 2018. Propofol Induces Nuclear Localization of Nrf2 under Conditions of Oxidative Stress in Cardiac H9c2 Cells. vol. 13 e0196191.
Siegel, R.L., et al., 2017. Cancer statistics, 2017. CA Cancer J. Clin. 67, 7–30.
Tano, K., Akimitsu, N., 2012. Long non-coding RNAs in cancer progression. Front. Genet. 3, 219.
Voutilainen, P.E., et al., 2001. Prognosis after lymph node recurrence in papillary thyroid carcinoma depends on age. Thyroid 11, 953–957.
Wang, H., et al., 2018a. Propofol prevents the progression of malignant pheochromocytoma in Vitro and in Vivo. DNA Cell Biol. 37, 308–315.
Wang, X.M., et al., 2018b. LncRNA PTCSC3 affects drug resistance of anaplastic thyroid cancer through STAT3/INO80 pathway. Cancer Biol. Ther. 19, 590–597.
Xu, Y.B., et al., 2013. Propofol suppresses proliferation, invasion and angiogenesis by down-regulating ERK-VEGF/MMP-9 signaling in Eca-109 esophageal squamous cell carcinoma cells. Eur. Rev. Med. Pharmacol. Sci. 17, 2486–2494.
Xu, S.T., et al., 2017. Long non-coding RNA ANRIL promotes carcinogenesis via sponging miR-199a in triple-negative breast cancer. Biomed. Pharmacother. 96, 14–21.
Xu, K., et al., 2018. Propofol prevents IL-13-induced epithelial-mesenchymal transition in human colorectal cancer cells. Cell Biol. Int. 42, 985–993.
Yang, L., et al., 2017. Long non-coding RNAs involved in autophagy regulation. Cell Death Dis. 8, e3073.
Yu, B., et al., 2018. Propofol induces apoptosis of breast cancer cells by downregulation of miR-24 signal pathway. Cancer Biomark. 21, 513–519.
Zhang, D., et al., 2015. Propofol promotes cell apoptosis via inhibiting HOTAIR mediated mTOR pathway in cervical cancer. Biochem. Biophys. Res. Commun. 468, 561–567.
Zhang, Z., et al., 2018. ANRIL promotes chemoresistance via disturbing expression of ABCC1 by regulating the expression of Let-7a in colorectal cancer. Biosci. Rep. 38https://doi.org/10.1042/BSR20180620. pii: BSR20180620.
Zhao, H., Zhang, X., 2018. Propofol protects rat cardiomyocytes from anthracycline-induced apoptosis by regulating MicroRNA-181a in vitro and in vivo. pp. 2109216.
Zhao, J.J., et al., 2016. Long non-coding RNA ANRIL promotes the invasion and metastasis of thyroid cancer cells through TGF-beta/Smad signaling pathway. Oncotarget 7, 57903–57918.
Zhao, B., et al., 2018. Overexpression of lncRNA ANRIL promoted the proliferation and migration of prostate cancer cells via regulating let-7a/TGF-beta1/Smad signaling pathway. Cancer Biomark. 21, 613–620.